Available online at www.sciencedirect.com
SCIENCE DIRECT®
Biochemical and Biophysical Research Communications 338 (2005) 584–589
BBRC
www.elsevier.com/locate/ybbrc

Evidence for the hydrophobic cavity of heme oxygenase-1 to be a CO-trapping site

Catharina T. Migita [a,*], Satoko Togashi [a], Miki Minakawa [a], Xuhong Zhang [b], Tadashi Yoshida [b,*]

[a] *Department of Biological Chemistry, Faculty of Agriculture, Yamaguchi University, Yamaguchi, Japan*
[b] *Department of Biochemistry, Yamagata University School of Medicine, Yamagata, Japan*

Received 19 July 2005
Available online 18 August 2005

Abstract

Carbon monoxide (CO) is produced during the heme catabolism by heme oxygenase. In brain or blood vessels, CO functions as a neurotransmitter or an endothelial-derived relaxing factor. To verify whether crystallographically proposed CO-trapping sites of rat and cyanobacterial heme oxygenase-1 really work, heme catabolism by heme oxygenase-1 from rat and cyanobacterial *Synechocystis* sp. PCC 6803 has been scrutinized in the presence of 2-propanol. If 2-propanol occupies the trapping sites, formation of CO-bound verdoheme should be enhanced. Although effects of 2-propanol on the rat heme oxygenase-1 reaction were obscure, the reaction of cyanobacterial enzyme in the presence of NADPH/ferredoxin reductase/ferredoxin was apparently affected. Relative amount of CO-verdoheme versus CO-free verdoheme detected by optical absorption spectra increased as the equivalent of 2-propanol increased, thereby supporting indirectly that the hydrophobic cavity in cyanobacterial enzyme traps CO to reduce CO inhibition of verdoheme degradation.

Keywords: Heme oxygenase; Heme degradation; Verdoheme conversion; CO-trapping site; CO inhibition; Kinetics

A simple gaseous molecule, carbon monoxide, is endogenously generated in biological systems by heme oxygenase (HO), during the catabolism of hemin (ferric protoporphyrin IX) [1,2]. In mammals, two isoforms, a 33 kDa inducible HO-1 and a 36 kDa constitutive HO-2, play this role. Various physiological functions of endogenous CO have been suggested in mammalian systems. The in vivo produced CO stimulates soluble guanylyl cyclase to form cGMP [3]. CO works as a neurotransmitter akin to NO in the brain and peripheral autonomic nerve system [4], functions as an endothelial-derived relaxing factor [5], and operates as a coneurotransmitter with nitric oxide in the gastrointestinal pathway [6,7]. Active HO proteins of other biological species have also been obtained and are known to produce CO [8–13] but physiological roles of endogenous CO in such species yet remain to be clarified.

Mechanism of the CO production, i.e., chemistry of the heme degradation by HO, has been characterized mostly using mammalian enzymes [14,15]. HO-1 complexed with one equivalent of hemin binds an oxygen molecule on the reduced heme iron [16,17] in the presence of electrons supplied by NADPH-cytochrome P450 reductase (CPR) [18]. The active form of the heme degradation is hydroperoxylhemin [19], which starts the three-step successive self-mono-oxygenation and degradation of the porphyrin ring. First, the hydroperoxylhemin spontaneously converts to α-*meso*-hydroxylhemin keeping strict α-regioselectivity and second, the hydroxylated

* Corresponding authors. Fax: +81 83 933 5863 (C.T. Migata), +81 236 28 5225 (T. Yoshida).
E-mail addresses: ctmigita@yamaguchi-u.ac.jp (C.T. Migita), tyosida@med.id.yamagata-u.ac.jp (T. Yoshida).

0006-291X/$ - see front matter © 2005 Elsevier Inc. All rights reserved.
doi:10.1016/j.bbrc.2005.08.045

α-*meso* carbon is released as CO to form verdoheme [2] by consuming one electron and an oxygen molecule [20]. The verdoheme is further oxygenated and ring-opened to ferric biliverdin IX_α at the expense of three electrons and an oxygen molecule. Mechanism of the heme degradation by cyanobacterial HO-1 (Syn HO-1) is similar to that by mammalian enzymes other than that electrons are supplied by reduced ferredoxin (Fd) coupled with NADPH/ferredoxin reductase (FNR) [21]. Overall reaction from hemin to ferric biliverdin IX_α is illustrated in Scheme 1.

In the HO reaction, hemin and the two intermediates, α-*meso*-hydroxyheme and verdoheme, participate in oxygen activation. Although the ferrous state of these three substrates can bind CO, the overall reaction is not severely inhibited by the endogenous CO. This is, partly because, affinity of the ferrous ion of heme for molecular oxygen is extremely high and the iron of α-*meso*-hydroxyheme does not participate in oxygen activation. Further, CO binding to the verdoheme-HO complex is relatively weak and the dissociation constant of CO is large [22].

Meanwhile, recent crystallographic analysis on the CO-bound rat heme-HO-1 (rHO-1) crystal has proposed that CO-trapping site(s) exists in rHO-1 [23], which transiently holds CO and assists its escape from the heme pocket. The CO-trapping site is among the hydrophobic cluster adjacent to the heme pocket, in the α-*meso* direction of the bound heme (Fig. 1A). Similar cavity has been found among the corresponding hydrophobic region of Syn HO-1 complexed with hemin in crystal, which is occupied by a 2-propanol molecule used for the crystallization (Fig. 1B) [24].

These observations prompted us to investigate whether such hydrophobic cavity actually works as a CO-trapper, so as CO not to coordinate on verdoheme and to assist in extrusion of CO from the heme pocket.

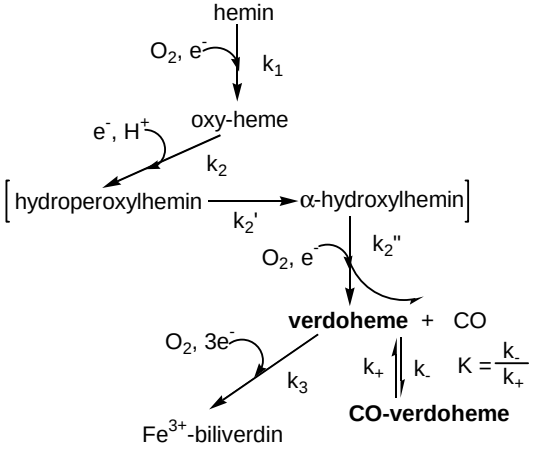

Scheme 1. Reaction mechanisms of the hemin degradation by heme oxygenase.

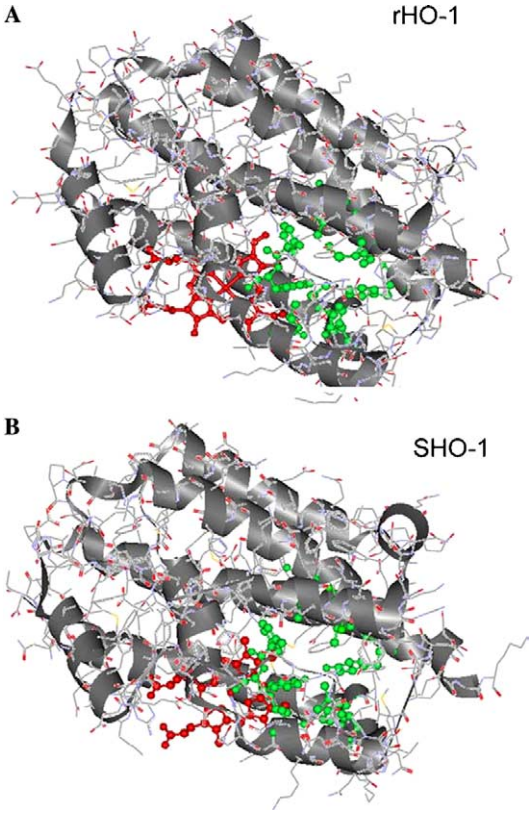

Fig. 1. Structure of the proposed CO-trapping sites. Cavities are surrounded by M34, F37, F47, V50, M51, L54, L147, F166, and F167 in rHO-1[18] and by V26, F29, Y39, L42, V43, L46, L138, F155, and Y156 in Syn HO-1[19], colored green. Hemes are colored red.

In this study, we tried to fill the cavity with 2-propanol by incubating heme-rat HO-1 or heme-Syn HO-1 in buffer solutions containing appropriate equivalents of 2-propanol. Then, relative amounts of CO-verdoheme versus (CO-free) verdoheme produced transiently during the heme degradation were compared between the HO-1 reactions with and without 2-propanol. As a result, in the heme conversion reactions by Syn HO-1 coupled with NADPH/FNR/Fd, obvious increase of the relative amount of CO-verdoheme to verdoheme was detected depending on the concentration of 2-propanol.

Materials and methods

Construction of expression plasmid of a truncated form of human cytochrome P450 reductase (ΔCPR). Human CPR is bound to microsomal membrane with an N-terminal hydrophobic region. To obtain a soluble, catalytically active enzyme, we constructed an expression plasmid of human CPR without the first 50 amino acid residues (ΔCPR) by PCR. The cDNA of human CPR as a template is a gift from Dr. F. Gonzalez of NIH [25]. A pair of synthetic oligonucleotides (FCPR and RCPR) was used as primers. FCPR (5′-TG GTTCCTCTTCAGACATATGAAAGAAGAAGTCCCC-3′) corresponds to the nucleotide sequence of human CPR from positions 130 to 165, except that AAGAAA at positions 145–150 was replaced by CATATG underlined. The underlined 5′-CATATG-3′ represents the

*Nde*I recognition site involving an initiation codon. RCPR (3′-CT GCACACCTCGATTCGAAGACGGACGGGGTGGGTG-5′) corresponds to the complementary nucleotide sequence of human CPR from positions 2029 to 2064, except that ATCCCCG at positions 2041–2047 was replaced by ATTCGAA underlined. The sequences of 3′-ATT-5′ and 3′-TTCGAA-5′ are the complementary sequences of a stop codon and the *Hin*dIII recognition site, respectively. The PCR products were digested with *Nde*I and *Hin*dIII, and then ligated into the *Nde*I and *Hin*dIII sites of the pMW172 expression vector.

Expression and purification of proteins. Recombinant Syn HO-1 and a truncated form of rHO-1 were expressed and purified by the same methods described previously [11,26]. Reconstitution of hemin to these HO-1s was also performed by the described method. Maize Fd type III and NADPH/FNR were expressed and purified according to the published methods [27,28].

Preparation of a soluble fraction of *Escherichia coli* cells containing CPR was performed similar to that for Syn HO-1 [11]. The precipitate obtained from the soluble fraction at 40–65% saturation of ammonium sulfate was suspended in 15 volumes (15 ml per gram of *E. coli* cells) of 20 mM potassium-phosphate buffer (KPB) (pH 7.4). The suspension was applied to a DE-52 column (2.6 × 30 cm) and the protein was eluted with a 400 ml linear gradient of 100–400 mM KCl in 20 mM KPB (pH 7.4). Yellow fractions with an intense 72 kDa band on SDS–PAGE were pooled and then loaded on a column of hydroxyapatite (2.6 × 20 cm). The protein was eluted with a 400 ml linear gradient of 20–300 mM KPB (pH 7.4) and the yellow eluate was loaded on a column of 2′5′-ADP Sepharose 4B (2 × 5 cm, Amersham Pharmacia Biotech). The column was washed with 50 ml of 0.1 M KPB (pH 7.4), and CPR was eluted with 20 ml of 0.1 M KPB (pH 7.4) containing 7 mg/ml 2′(3′)-AMP (Sigma). Finally, the 2′(3′)-AMP in the eluate was removed by passage through a Sephadex G-25 column equilibrated with 0.1 M KPB (pH 7.0). The final products were stored in 50% glycerol at −80 °C until use.

Assessment of effects of 2-propanol on the heme degradation by rHO-1 and Syn HO-1. All the HO-1 complexes were prepared in 5 μM solutions of 0.1 M KPB (pH 7.0). 2-Propanol was added by 0–3000 equivalents into the solution of heme-Syn HO-1 or heme-rHO-1. Mixtures prepared were incubated for 30 min on ice prior to the measurement of optical absorption spectra. To each solution, appropriate reducing equivalents, sodium ascorbate (1000 equiv versus heme HO-1) or NADPH (3 equiv to the rHO-1 solutions containing CPR and 4 equiv for the Syn HO-1 solutions containing FNR and Fd) was supplied to start the reaction. Recording of the optical absorption spectra and kinetic measurements were performed on a Shimadzu UV-2200 spectrophotometer at 25 °C.

Results and discussion

Effect of 2-propanol on ascorbate-assisted heme degradation by HO-1

The heme conversion reaction by Syn HO-1 in the presence of 1000 equiv of ascorbate proceeds as shown in Fig. 2. This reaction is over 20 times slower than the NADPH/FNR/Fd coupled reaction described later. In the ascorbate-supported Syn HO-1 reaction, characteristic α- and β-bands of the oxy-heme complex are hardly seen and during 3–30 min after the initiation of the reaction small bands of CO-verdoheme and verdoheme appear at 640 and 688 nm, respectively. These bands are gradually diminished and replaced by a broad absorption band of free biliverdin appearing around this region. The ascorbate-supported reaction by rHO-1 occurs 10 times faster than the Syn HO-1 reaction, showing small α- and β-bands of oxy-heme at 576 and 536 nm, respectively, and small bands of CO-verdoheme and verdoheme at 637 and 688 nm are also observed (data not shown). The same ascorbate-supported reactions by Syn HO-1 and rHO-1 were conducted in the presence of 10, 50, 100, 500, 1000, and 3000 equiv of 2-propanol but noticeable differences were not observed in optical spectra recorded at the same time courses as shown in Fig. 2. In Fig. 3, apparent initial velocities of the heme degradation are plotted against the equivalent of 2-propanol. This result shows that 10–3000 equiv of

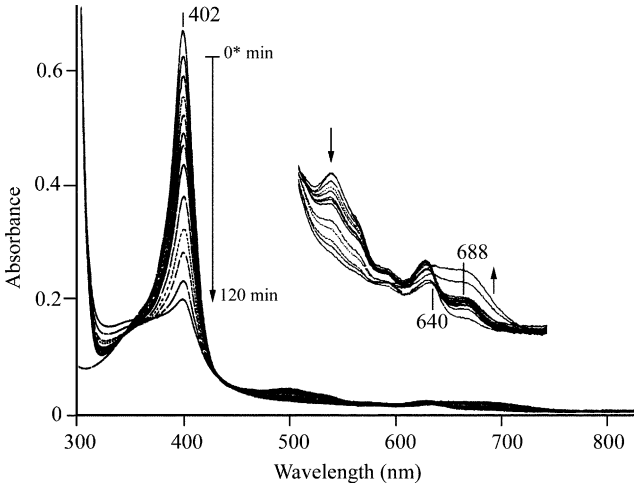

Fig. 2. Heme-degradation reaction by Syn HO-1 with ascorbate. The spectra were recorded before the addition of ascorbate, immediately after the addition of 1000 equiv of ascorbate (denoted as 0* min), and after 3–15 min with 3-min intervals, and after 20, 30, 45, 60, 90, and 120 min. The visible region is expanded for the spectrum recorded at the same time courses.

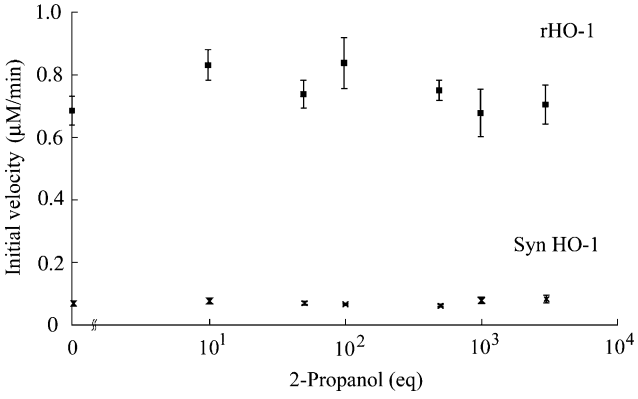

Fig. 3. Plots of initial velocity of hemin degradation versus equivalent of 2-propanol mixed in buffer solutions. The initial velocity (mean values ± SEM) is estimated as decreasing rates of the ferric heme complex by monitoring a decrease of absorbance at 402 nm with $\varepsilon = 128\ \mathrm{mM^{-1}\,cm^{-1}}$ for the Syn HO-1 complex and at 405 nm with $\varepsilon = 140\ \mathrm{mM^{-1}\,cm^{-1}}$ for the rHO-1 complex.

2-propanol does not change the initial velocity of heme degradation either by Syn HO-1 or by rHO-1.

As evidenced by the spectra exhibiting no distinct bands of the oxy-heme (Fig. 2), the reduction of hemin (k_1) is slower than the degradation of the oxy-heme (k_2). That is, the k_1 restricts verdoheme formation (Scheme 1) in such slow reactions, unlike in mammalian HO-1 reactions coupled with NADPH/CPR where k_3 restricts the overall reaction [29]. Then, the steady-state concentration of verdoheme and CO-verdoheme is restricted by k_1, k_3, and K. Fig. 2 shows that the absorption peaks of CO-verdoheme (640 nm) and verdoheme (688 nm) are small and during 3–20 min after the initiation of the reaction they keep nearly the same height, suggesting that the rate of verdoheme formation is slightly faster than its degradation and the concentration of verdoheme and CO-verdoheme is nearly in a steady state. In such quasi-steady-state condition, increase of CO due to inhibition of the CO-trapping with the hydrophobic cavity by 2-propanol could not affect the equilibrium, written with the equilibrium constant K in Scheme 1, significantly.

Effect of 2-propanol on heme-HO-1 reactions under physiological electron donating systems

Heme degradations by HO coupled with physiological electron donating systems, i.e., 4 equiv of NADPH with FNR (0.05 equiv) and Fd (0.5 equiv) for Syn HO-1 and 3 equiv of NADPH with CPR (0.02 equiv) for rHO-1, occur much faster than the ascorbate-assisted reactions (Fig. 4). Since prominent absorption bands of oxy-heme are observed in both reactions (at 535 and 575 nm in Fig. 4A and at 539 and 576 nm in Fig. 4B), k_1 is known to be much larger than k_2, so that formation of verdoheme is restricted by k_2, k_3, and K (Scheme 1). Due to the accelerated verdoheme formation, transiently detected absorption bands of verdoheme and CO-verdoheme are both increased (Fig. 4) compared with those in the ascorbate-supported reactions (Fig. 2). In the Syn HO-1 reaction shown in Fig. 4A, the verdoheme band (at 688 nm) appears to be much larger than the CO-verdoheme band (at 640 nm) immediately after initiation of the reaction, denoted as at 0* min. In the following 2 min, both bands are amplified to the maxima. Here, we define the increment of absorbance of the CO-verdoheme band at 640 nm and that of the verdoheme band at 688 nm for initial 2 min of the reaction as Δ640 and Δ688, respectively. Then, in the Syn HO-1 reaction, Δ640 is larger than Δ688. Similar increase of the bands of CO-verdoheme (637 nm) and verdoheme (688 nm) during the same reaction interval is observed in the rHO-1 reaction (Fig. 4B), however, in this case, Δ637 is almost equal to Δ688.

Next, we compared Δ640 to Δ688 or Δ637 to Δ688 observed in the Syn HO-1 or rHO-1 reactions conducted

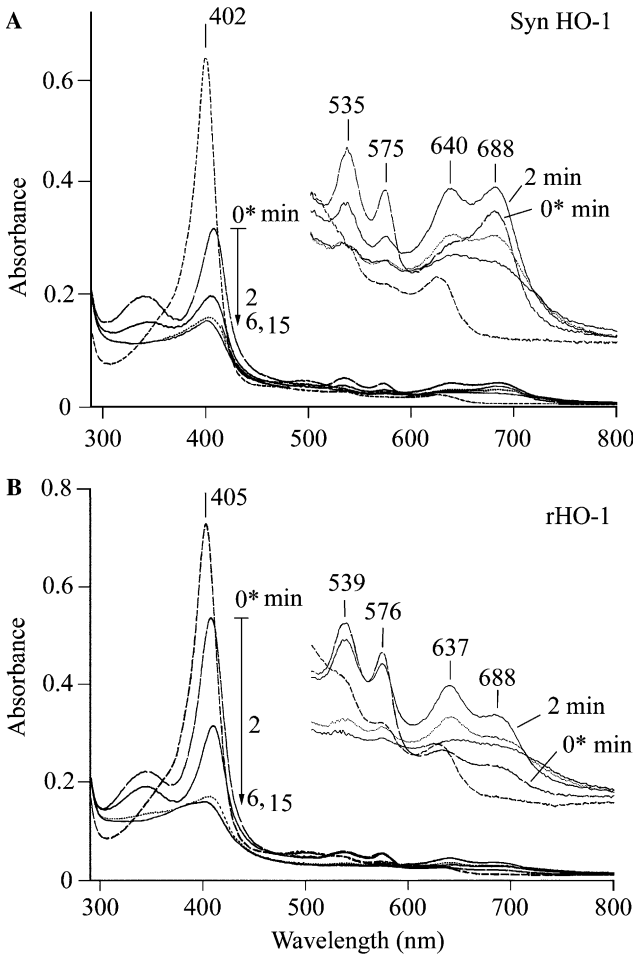

Fig. 4. Heme degradation reaction by Syn HO-1 (A) and rHO-1 (B) using electrons from NADPH coupled with FNR/Fd for (A) and CPR for (B). The spectra were recorded before the addition of NADPH, immediately after the addition of NADPH (denoted as 0* min), and 2, 6, and 15 min after the addition of NADPH.

with different initial rates, by changing the equivalent of Fd or CPR for the Syn HO-1 and the rHO-1 reactions, respectively. Fig. 5 exhibits visible regions of the spectra recorded at 0* min and 2 min after the initiation of heme degradation by Syn HO-1 with NADPH/FNR/Fd (Spectra A and B) and by rHO-1 with NADPH/CPR (Spectra C and D). Here, the ratios of the apparent initial velocities of the reactions corresponding to the spectra A–D are roughly 3.3:2:4:1, as measured by the decreasing rate of each Soret band of the spectrum (data not shown). In relatively faster reactions giving spectra of Figs. 5A and C, as plainly indicated by the faster decreases of the oxy-heme bands, differences between Δ640 and Δ688 or between Δ637 and Δ688 are distinct, while in the reactions giving spectra of Figs. 5B and D, Δ640 and Δ688 or Δ637 and Δ688 are similar. These results represent that acceleration of the verdoheme formation extends the lifetime of verdoheme and shifts the equilibrium (K in Scheme 1) toward CO-verdoheme formation, and such shifts manifest itself in Δ640/Δ688

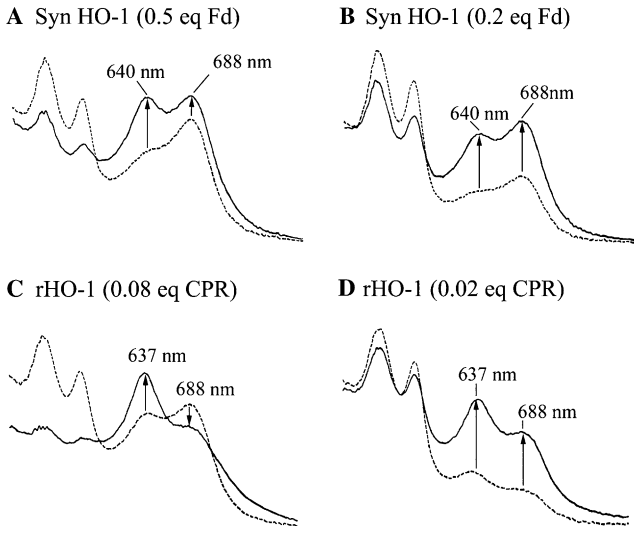

Fig. 5. Comparison of the characteristic absorption bands of CO-verdoheme and verdoheme obtained from the spectra recorded at 0* min (----) and 2 min (——) after the initiation of heme degradation. (A) and (B) for heme-Syn HO-1 (5 μM) with FNR (0.05 equiv), NADPH (4 equiv), and Fd (0.5 equiv for (A) and 0.2 equiv for (B)). (C) and (D) for heme-rHO-1 (5 μM) with NADPH (3 equiv) and CPR (0.08 equiv for (C) and 0.02 equiv for (D)). Allows indicated represent Δ640, Δ688, or Δ637, respectively.

or in Δ637/Δ688. Similarly, if 2-propanol inhibits competitively the CO-trapping by the hydrophobic cavity in HO, a shift of the equilibrium to the CO-verdoheme formation is likely to be observed due to extension of the lifetime of CO.

We conducted heme degradation reactions by Syn HO-1 in the presence of 25, 50, 100, and 500 equiv of 2-propanol, coupled with NADPH/FNR/Fd. Two kinds of equivalents, 0.2 and 0.5, of Fd were applied, where the apparent initial velocity of the reaction using 0.2 equiv of Fd is 2/3 of that of the reaction with 0.5 equiv of Fd. Similar experiments were also performed for the rHO-1 reaction with NADPH/CPR in the presence of 2-propanol. For each reaction, the optical absorption spectrum recorded at 0* min was compared with that recorded after 2 min and the ratios of Δ640/Δ688 or Δ637/Δ688 were estimated from the increments of each absorption band during this reaction interval. Obvious effect of 2-propanol is found for the faster reaction of Syn HO-1 conducted with 0.5 equiv of Fd and small effect also detected for the rHO-1 reaction (Fig. 6). In the faster Syn HO-1 reaction, the value of Δ640/Δ688 is at the maximum in the presence of 50 equiv of 2-propanol. In the presence of 2-propanol over 100 equiv, this ratio decreases and total amounts of CO-verdoheme plus verdoheme also reduce, suggesting that the heme degradation is somewhat retarded by a large amount of 2-propanol, though the ascorbate-supported Syn HO-1 reaction is not affected by 2-propanol (Fig. 3). Far excess 2-propanol might interfere with the electron transfer from Fd to Syn HO-1.

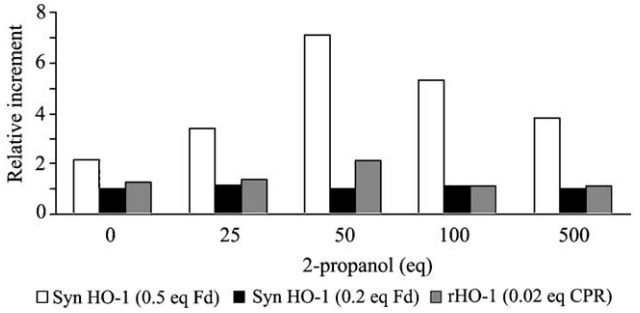

Fig. 6. The comparison of the relative increment, Δ640/Δ688 or Δ637/Δ688, of CO-verdoheme formation depending on the added equivalent of 2-propanol. Δ640 and Δ688 represent increments of absorbance at 640 and 688 nm for initial 2 min of the heme conversion reaction by Syn HO-1, respectively. Δ637 and Δ688 are the corresponding values for the rHO-1 reactions.

By comparing the spectra recorded at 0* min (dotted line) shown in Fig. 5, it is clear that relative heights of the CO-verdoheme band (at 637 nm) to the verdoheme band (at 688 nm) obtained for the rHO-1 reactions (Figs. 5C and D) are larger than those of corresponding bands in Figs. 5A and B for Syn HO-1 reactions. This indicates that in the rHO-1 reactions, more CO-verdoheme is produced immediately after initiation of the reactions than in the Syn HO-1 reactions. Therefore, affinity of verdoheme to CO seems to be relatively high in rHO-1. The crystallographic analysis of heme-rHO-1 suggests that the heme pocket of rHO-1 is more polar than that of Syn HO-1 [24]. The polar heme pocket could stabilize CO coordination on verdoheme and lead to the high CO affinity of verdoheme. If that were the case, CO-trapping by the distal protein cavity of rHO-1 might be intrinsically less effective than that by Syn HO-1 cavity.

Conclusive remarks

2-Propanol mixed in the buffer solutions of heme-Syn HO-1 affects the ratio of the amounts of CO-verdoheme/verdoheme produced during the heme degradation. The 50–100 eqs of 2-propanol amplify the ratio of increments of absorbance at 640 nm (CO-verdoheme) versus that at 688 nm (verdoheme), Δ640/Δ688, during the first 2 min of the reaction by 3–4 times compared with the ratio obtained in the reaction without 2-propanol. This effect manifests itself when velocity of the verdoheme production is far fast against that of verdoheme degradation, as a result of a shift of equilibrium to the CO-verdoheme formation. This observation supports the possibility that the proposed hydrophobic cavity of Syn HO-1 works as a CO-trapping site. The rHO-1 reaction, however, is not apparently affected by the presence of 2-propanol, probably because the affinity of verdoheme to CO in rHO-1 is higher than that in Syn HO-1.

Acknowledgments

The bacterial expression vector pMW 172 is a gift from Dr. K. Nagai, MRC Laboratory of Molecular Biology, Cambridge, UK. *E. coli* expression plasmids for maize FNR and Fd type III are gifts from Professor T. Hase, Osaka University. This work was partly supported by a Grant-in-Aid for Scientific Research (16570108) to T.Y. from the Ministry of Education, Culture, Sports, Science and Technology, Japan.

References

[1] R. Tenhunen, H.S. Marver, R. Schmid, The enzymatic conversion of heme to bilirubin by microsomal heme oxygenase, Proc. Natl. Acad. Sci. USA 61 (1968) 748–755.
[2] T. Yoshida, M. Noguchi, G. Kikuchi, The step of carbon monoxide liberation in the sequence of heme degradation catalyzed by the reconstituted microsomal heme oxygenase system, J. Biol. Chem. 257 (1982) 9345–9348.
[3] P. Vigne, E. Feolde, A. Ladoux, D. Duval, C. Frelin, Contributions of NO synthase and heme oxygenase to cGMP formation by cytokine and hemin-treated brain capillary endothelial cells, Biochem. Biophys. Res. Commun. 214 (1995) 1–5.
[4] L. Xue, G. Farrugia, S.M. Miller, C.D. Ferris, S.H. Snyder, J.H. Szurszewski, Carbon monoxide and nitric oxide as coneurotransmitters in the enteric nervous system: evidence from genomic deletion of biosynthetic enzymes, Proc. Natl. Acad. Sci. USA 97 (2000) 1851–1855.
[5] M. Suematsu, S. Kashiwagi, T. Sano, N. Goda, Y. Shinoda, Y. Ishimura, Carbon monoxide as an endogenous modulator of hepatic vascular perfusion, Biochem. Biophys. Res. Commun. 205 (1994) 1333–1337.
[6] R. Zakhary, K.D. Poss, S.R. Jaffrey, C.D. Ferris, S. Tonegawa, S.H. Snyder, Targeted gene deletion of heme oxygenase2 reveals neural role for carbon monoxide, Proc. Natl. Acad. Sci. USA 94 (1997) 13853–14848.
[7] D.E. Barañano, S.H. Snyder, Neural roles for heme oxygenase: contrasts to nitric oxide synthase, Proc. Natl. Acad. Sci. USA 98 (2001) 10996–11002.
[8] A. Wilks, M.P. Schmitt, Expression and characterization of a heme oxygenase (Hmu O) from *Corynebacterium diphtheriae*, J. Biol. Chem. 273 (1998) 837–841.
[9] W. Zhu, A. Wilks, I. Stojiljkovic, Degradation of heme in Gram-negative bacteria: the product of the *hem O* gene of Neisseriae is a heme oxygenase, J. Bacteriol. 182 (2000) 6783–6790.
[10] T. Muramoto, N. Tsurui, M.J. Terry, A. Yokota, T. Kohchi, Expression and biochemical properties of a ferredoxin-dependent heme oxygenase required for phytochrome chromophore synthesis, Plant Physiol. 130 (2002) 1958–1966.
[11] C.T. Migita, X. Zhang, T. Yoshida, Expression and characterization of cyanobacterium heme oxygenase, a key enzyme in the phycobilin synthesis: properties of the heme complex of recombinant active enzyme, Eur. J. Biochem. 270 (2003) 687–698.
[12] X. Zhang, M. Sato, M. Sasahara, C.T. Migita, T. Yoshida, Unique features of recombinant heme oxygenase of *Drosophila melanogaster* compared with those of other heme oxygenases studied, Eur. J. Biochem. 271 (2004) 1713–1714.
[13] X. Zhang, C.T. Migita, M. Sato, M. Sasahara, T. Yoshida, Protein expressed by the *ho2* gene of the cyanobacterium *Synechocystis* sp. PCC 6803 is a true heme oxygenase—properties of the heme and enzyme complex, FEBS J. 272 (2005) 1012–1022.
[14] T. Yoshida, C.T. Migita, Mechanism of heme degradation by heme oxygenase, J. Inorg. Biochem. 82 (2000) 33–41.
[15] C. Colas, P.R. Ortiz de Montellano, Autocatalytic radical reactions in physiological prosthetic heme modification, Chem. Rev. 103 (2003) 2305–2332.
[16] T. Yoshida, G. Kikuchi, Purification and properties of heme oxygenase from pig spleen microsomes, J. Biol. Chem. 253 (1978) 4224–4229.
[17] T. Yoshida, G. Kikuchi, Features of the reaction of heme degradation catalyzed by the reconstituted microsomal heme oxygenase system, J. Biol. Chem. 253 (1978) 4230–4236.
[18] B.A. Schacter, E.B. Nelson, H.S. Marver, B.S.S. Masters, Immunochemical evidence for an association of heme oxygenase with the microsomal electron transport system, J. Biol. Chem. 253 (1972) 3601–3607.
[19] R. Davydov, U. Fofman, H. Fujii, T. Yoshida, M. Ikeda-Saito, B.M. Hoffman, Catalytic mechanism of heme oxygenase through EPR and ENDOR of cryoreduced oxy-heme oxygenase and its Asp 140 mutant, J. Am. Chem. Soc. 124 (2002) 1798–1808.
[20] K. Mansfield Matera, S. Takahashi, H. Fujii, H. Zhou, K. Ishikawa, K.T. Yoshimura, D.L. Rousseau, T. Yoshida, M. Ikeda-Saito, Oxygen and one reducing equivalent are both required for the conversion of α-hydroxyhemin to verdoheme in heme oxygenase, J. Biol. Chem. 271 (1996) 6618–6624.
[21] J. Cornejo, R.D. Willows, S.I. Beale, Phytobilin biosynthesis:cloning and expression of a gene encoding soluble ferredoxin-dependent heme oxygenase from *Synechocystis* sp. PCC 6803, Plant J. 15 (1998) 99–107.
[22] C.T. Migita, K. Mansfield Matera, M. Ikeda-Saito, J.S. Olson, H. Fujii, T. Yoshimura, H. Zhou, T. Yoshida, The oxygen and carbon monoxide reactions of heme oxygenase, J. Biol. Chem. 273 (1998) 945–949.
[23] M. Sugishima, H. Sakamoto, M. Noguchi, K. Fukuyama, CO-trapping site in heme oxygenase revealed by photolysis of its CO-bound heme complex: mechanism of escaping from product inhibition, J. Mol. Biol. 341 (2004) 7–13.
[24] M. Sugishima, C.T. Migita, X. Zhang, T. Yoshida, K. Fukuyama, Crystal structure of heme oxygenase-1 from cyanobacterium *Synechocystis* sp. PCC 6803 in complex with heme, Eur. J. Biochem. 271 (2004) 4517–4525.
[25] S. Yamano, O.W. McBride, J.P. Hardwick, H.V. Gelboin, F.J. Gonzalez, Human NADPH-P450 oxidoreductase: complementary DNA cloning, sequence and vaccina virus-mediated expression and localization of the CYPOR gene to chromosome 7, Mol. Pharmacol. 36 (1989) 83–88.
[26] K. Mansfield Matera, H. Zhou, C.T. Migita, S.E. Hobert, K. Ishikawa, K. Katakura, H. Maeshita, T. Yoshida, M. Ikeda-Saito, Histidine-132 does not stabilize a distal water ligand and is not an important residue for the enzyme activity in heme oxygenase-1, Biochemistry 36 (1997) 4909–4915.
[27] T. Hase, S. Mizutani, Y. Mukohata, Expression of maize ferredoxin cDNA in *Escherichia coli*, Plant Physiol. 97 (1991) 1395–1401.
[28] Y. Onda, T. Matsumura, Y. Kimata-Ariga, H. Sakakibara, T. Sugiyama, T. Hase, Differential interaction of maize root ferredoxin: $NADP^+$ oxidoreductase with photosynthetic and non-photosynthetic ferredoxin isoproteins, Plant Physiol. 123 (2000) 1037–1045.
[29] Y. Liu, P.O. OrtizdeMotellano, Reaction intermediates and single turnover rate constants for the oxidation of heme by human heme oxygenase-1, J. Biol. Chem. 275 (2000) 5297–5307.